Mine Water Environ (2009) 28:253–263
DOI 10.1007/s10230-009-0080-x

TECHNICAL ARTICLE

Treatment of an Iron-rich ARD Using Waste Carbonate Rock: Bench-Scale Reactor Test Results

Daniel Ray · Malcolm Clark · Tracey Pitman

Received: 19 May 2009 / Accepted: 22 June 2009 / Published online: 10 July 2009

Abstract The treatment of acid rock drainage (ARD) places extraordinary financial burdens on governments and companies worldwide, and an improved efficiency in treatment by as little as 1% can save many millions of dollars in rehabilitation. We investigated a system for treating Fe-rich ARD using a three-stage reactor design. In the first reaction cell, Fe-rich ARD was partially neutralised using rapid periodic carbonate resuspension with a rotating axial mixer. This was followed by an air-sparged oxidation chamber and then a second reaction cell, with more carbonate periodically resuspended until a pH of 6.3 was reached, which was followed by a settlement chamber. This reactor design has a high capacity for neutralisation, with an efficiency of ≈70% of acidity neutralised by the acid neutralising capacity (g of $CaCO_3$ equivalent) added to the reactor. Axial mixers were tested because of their low-energy requirements and their high reliability. The intermediate chamber effectively removes Fe by oxidising Fe(II) to Fe(III). Given the amount of acidity neutralised, the sludge volume produced was low compared to other technologies, providing further potential savings in sludge handling. Waste carbonate rock proved to be an effective neutralising agent, even though it was about 60% dolomite and 40% magnesite, with minor calcite, and despite the fact that magnesite has substantially slower dissolution kinetics compared to the more dominant dolomite. The mixed waste carbonates were capable of raising the pH sufficiently to reduce the heavy metal loadings in Fe-rich ARD by more than two orders of magnitude. The final settlement stage of the process was shown to be essential for metal precipitation, for the carry-over of fine carbonates, and CO_2 loss. This was associated with a rise in pH, from 6.3 to 7.5. In addition, residual slow-reacting magnesite from the mixed carbonate remains in the sludge from the first reactor and provides acid buffering capacity within the sludge, which is commonly lacking in the ARD neutralisation sludge of other systems.

Keywords Axial mixed · Carbonate neutralisation · Fe-rich · Multi-staged treatments · Oxidative-precipitation

D. Ray · T. Pitman
Department of Tourism, Arts and the Environment, Tasmania, GPO Box 1751, Hobart, TAS 7001, Australia

M. Clark (✉)
Centre for Coastal Management, Southern Cross University, PO Box 5125, East Lismore, NSW 2480, Australia
e-mail: malcolm.clark@scu.edu.au; mclark@scu.edu.au

D. Ray
Aquatic Science, 122 Karratha Dr, Sandford, TAS 7020, Australia

Introduction

The mining sector spends more on the management of acid rock drainage (ARD) and sulphidic tailings than any other environmental management issue. Management of ARD in Australia alone is estimated to cost at least AUS $60 million per annum (Harries 1997). Globally, the liability is estimated to be well in excess of US $30 billion annually (Taylor 1999). Given this cost and the complexity of ARD remediation, there is an opportunity for large cost savings through evolution of ARD management strategies. In addition, although management of ARD can be required for decades (Parker and Robertson 1999) after mine closure and at historic mine-sites, it is more costly at such sites because of the loss of operating infrastructure (Harries 1997). Pre-empting the problem by controlling the

formation and/or escape of ARD is therefore best practice of environmental management in modern mining operations (Parker and Robertson 1999). However, remediation and treatment of ARD remains an important management tool because prevention is not always achieved, nor is it always practical, especially at historic sites where the legacy already exists (Johnson and Hallberg 2005).

Efficient and effective treatment of ARD is complex and site-specific, requiring evaluation of environmental, site geochemical, social, and economic factors (Parker and Robertson 1999). Treatment strategies may be abiotic (aeration, neutralisation or alkaline drains), or biotic (bioreactors, wetlands, or permeable reactive barriers) (Johnson and Hallberg 2005). The site characteristics of the Savage River Mine generally favour abiotic over biotic treatments: it is in a wet temperate environment with steep topography, and without a ready source of carbon.

Although limestone (carbonate rock) neutralisation is the cheapest abiotic treatment available, it can be problematic due to its low solubility and armouring (Parker and Robertson 1999) and handling and disposal of the voluminous, low density sludge produced (Johnson and Hallberg 2005; Sibrell and Watten 2003). At many mine sites, waste carbonates and other alkaline rocks are often located near the acid-producing ore materials, especially in mafic and ultra-mafic provenances. This is true for Savage River (Tasmania, Australia); there are several deposits of carbonate rocks (including magnesite) adjacent to the main ultra-mafic zone containing the magnetite ore bodies. The carbonate rock is a waste product to Australian Bulk Minerals (ABM's) Savage River magnetite mining operations. This carbonate rock is a potential neutralising agent and it was envisaged that it would be feasible and cost effective to process this carbonate rock through the current Savage River grinding circuit to produce a fine-grained neutralising material.

Magnesite rates well for solubility (Ksp) and acid-neutralising-capacity (ANC) compared to other carbonate minerals commonly available for acid neutralisation, viz. soda-ash (Na_2CO_3), calcite or ag-lime ($CaCO_3$), and dolomite ($Ca,Mg(CO_3)_2$), siderite ($FeCO_3$), and ankerite ($Ca,Fe(CO_3)_2$) (Table 1). However, magnesite has much slower dissolution rates (Household et al. 1999) and furthermore, the dissolution rate of mixed carbonates, such as those found at Savage River, are not well defined. There have been some observations on individual dissolution rates for dolomites and magnesite (Stumm and Morgan 1996) and the dissolution kinetics of calcite has been well described (e.g. Berner and Morse 1974; Busenberg and Plummer 1986; Chou et al. 1989; Plummer et al. 1978). Typically, the dissolution rate of magnesite is three orders of magnitude slower than calcite, and dolomite is an order of magnitude slower (Stumm and Morgan 1996).

Armouring of carbonates is especially problematic in the treatment of ARD high in iron, and some authors (e.g. Koehnken and Ray 1999; Parker and Robertson 1999) recommend that carbonate be used only where the iron concentrations are <5 mg/L, less than 0.5% of the level used in this study. In contrast, others have worked to refine ARD lime neutralisation processes by minimising the armouring of carbonate (e.g. pulsed limestone bed reactors (Watten et al. 2004) or have focused on reducing the volume of sludge produced (e.g. high-density sludge processes (Johnson and Hallberg 2005). The formation of Fe-containing floc also limits the use of carbonate rock as a neutralising agent (Parker and Robertson 1999) and iron oxidation can be rate-limiting, in particular across the pH range from pH 4 to pH 7 (Dempsey et al. 2001) where nearly all ARD neutralisation occurs. An adequate supply of dissolved oxygen is required for Fe(II) oxidation to Fe(III). The reaction for this process is:

$$4Fe^{2+} + O_2 + 4H^+ \leftrightarrow 4Fe^{3+} + 2H_2O. \quad (1)$$

While this reaction is a consumer of acid (H^+) and may lead to a temporary increase in pH, the precipitation of ferric iron is acid producing:

Table 1 Reactivity of carbonate minerals in contact with 0.1 M HCl solution at room temperature (after Evangelou 2000)

Mineral	Reactivity	Max pH[a]	ANC, Mole/kg	Ksp of solubility[b]
Na_2CO_3	Very high	≈12	16.7	6.02×10^{-1}
$MgCO_3$	Moderate (slow to dissolve)	8–9.2 (max)	23.7	6.82×10^{-6}
$CaCO_3$	Moderate	8–9.2 (max)	20	3.36×10^{-9}
$(Ca,Mg)CO_3$	Weak (unless finely crushed)	≈8	21.7	$\approx 3.3 \times 10^{-10}$
$FeCO_3$	Extremely weak (Very weak even when finely powdered)	≈8	Up to 17.3[c]	3.13×10^{-11}
$(Ca,Fe)CO_3$	Extremely weak to un-reactive (even when finely crushed)	≈8	Up to 18.5[c]	–

[a] From Evangelou (2000)

[b] Data from Lide (2003)

[c] ANC depends on the remaining oxidation state of the Fe and the oxidation pathways and may be acid producing, acid neutral or acid consuming

$$Fe^{3+} + 3H_2O \leftrightarrow Fe(OH)_3(s) + 3H^+. \quad (2)$$

The net result of these two reactions is acid production:

$$4Fe^{2+} + O_2 + 10H_2O \leftrightarrow 4Fe(OH)_{3(s)} + 8H^+. \quad (3)$$

The kinetics of these reactions for homogenous abiotic oxidation of iron have been described by many authors, including Stumm and Morgan (1996), and can be expanded and expressed as:

$$r_{\text{abiotic(homo)}} = \frac{\partial[Fe^{2+}]}{\partial t} = \frac{-k_{\text{abiotic(homo)}}[Fe^{2+}][O_2]}{[H^+]^2} = \frac{-\left\{A_{\text{abiotic(homo)}} \exp\left(\frac{-E_{a,\text{abiotic(homo)}}}{RT}\right)\right\}[Fe^{2+}][O_2]}{[H^+]^2}. \quad (4)$$

This relationship holds true between about pH 4.5 and 7. At pH's higher than 7, the rate for abiotic oxidation is independent of pH (Kirby et al. 1999); when pH is lower than about 4.5, abiotic iron oxidation is negligible. Dempsey et al. (2001) and Johnson and Hallberg (2005) found that the oxidation rates for ponds and channel systems with pH between 5 and 7 was best described as a heterogeneous oxidation process where increased concentrations of ferrous iron and oxygen increase the rate of reaction, but so does the presence of Fe(III), as follows:

$$r_{\text{abiotic(hetero)}} = \frac{\partial[Fe^{2+}]}{\partial t} = \frac{-k_{\text{abiotic(hetero)}}[Fe^{3+}][Fe^{2+}][O_2]}{[H^+]} = \frac{-\left\{A_{\text{abiotic(hetero)}} \exp\left(\frac{-E_{a,\text{abiotic(hetero)}}}{RT}\right)\right\}[Fe^{3+}][Fe^{2+}][O_2]}{[H^+]}. \quad (5)$$

However, because both hetero- and homogeneous reactions can occur simultaneously, the overall abiotic reaction can be re-expressed (Dempsey et al. 2001) as:

$$r_{\text{abiotic}} = r_{\text{abiotic(homo)}} + r_{\text{abiotic(hetro)}} = \frac{-k_{\text{abiotic(homo)}}[Fe^{2+}][O_2]}{[H^+]^2} + \frac{-k_{\text{abiotic(hetero)}}[Fe^{3+}][Fe^{2+}][O_2]}{[H^+]} = \frac{\left(-k_{\text{abiotic(homo)}} + -k_{\text{abiotic(hetero)}}[Fe^{3+}][H^+]\right)[Fe^{2+}][O_2]}{[H^+]^2} = \frac{\left(-\left\{A_{\text{abiotic(homo)}} \exp\left(\frac{-E_{a,\text{abiotic(homo)}}}{RT}\right)\right\} + -\left\{A_{\text{abiotic(hetro)}} \exp\left(\frac{-E_{a,\text{abiotic(hetero)}}}{RT}\right)\right\}[Fe^{3+}][H^+]\right)[Fe^{2+}][O_2]}{[H^+]^2}. \quad (6)$$

Below about pH 5, bacterial oxidation of Fe(II) can play a dominant role in Fe(II) oxidation, though there is some uncertainty for the rate equation at pHs greater than about 3.5 (Pesic et al. 1989). The rate equation controlling biological oxidation of Fe(II) is expressed as:

$$r_{\text{bio}} = \frac{\partial[Fe^{2+}]}{\partial t} = -k_{\text{bio}} C_{\text{bact}}[Fe^{2+}]\rho O_2[H^+] = -\left\{A_{\text{bio}} \exp\left(\frac{-E_{a,\text{bio}}}{RT}\right)\right\} C_{\text{bact}}[Fe^{2+}]\rho O_2[H^+]. \quad (7)$$

By combining the abiotic oxidation rate and the biotic oxidation rate, the overall oxidation rate (Kirby et al. 1999) can be expressed as:

$$\left(\frac{\partial[Fe^{2+}]}{\partial t}\right)_{\text{Overall}} = -r_{\text{abiotic}} - r_{\text{bio}}. \quad (8)$$

Kirby et al. (1999) found a crossing point at about pH 5, which was influenced by the concentration of the bacteria in the water. However, these reaction rates do not take into account that the oxidation of Fe(II) can be catalysed by metals (especially Cu^{2+} and Co^{2+}) and by anions that form complexes with Fe(III) (e.g. HPO_4^{2-}), which can enhance the oxidation rate substantially (Stumm 1996). Despite these potential enhancements, the rate of Fe (II) oxidation is inversely proportional to the acid $[H^+]$ concentration, so that a rise in pH will cause an increase in the Fe(II) oxidation rate.

Some authors (e.g. Parker and Robertson 1999) recommend the exclusion of oxygen in Fe-rich ARD neutralisation to prevent armouring of calcites by Fe(III)-oxyhydroxides. However, the kinetics described above show that maintaining oxygen availability during neutralisation of iron-rich ARD is advantageous for Fe removal, assuming of course that armouring does not occur. Therefore, it can be envisaged that an oxidation chamber between two neutralisation stages at a pH above 4.5 will allow abiotic oxidation of Fe(II) to occur, though inevitable colonisation by bacteria and algae may allow additional biotic oxidation to also occur. Also, having the oxidation stage between two neutralisation stages allows the iron to be oxidised and precipitated prior to the second neutralisation stage, thus potentially preventing armouring. In this approach, the oxidation, which is also acid

producing, occurs prior to a pH adjustment, allowing a greater time for reaction with carbonate, and potentially better plant efficiency. Inclusion of an aeration step in active treatment of ARD has been described by others (e.g. Skousen et al. 1998). However, those systems used the more common method of dosing the carbonate into the ARD flow (Skousen et al. 2005), which allows large numbers of very small crystallites to form and typically leads to a low density sludge. Where an iron-rich sludge is produced, studies have shown that steps such as pre-conditioning the sludge, controlled dosing, and slower rates of neutralisation all improve sludge density. Sludge densities as low as 8% (wt/vol or 0.08 g/mL) are considered a poor result and densities ranging between 25 and 31% (wt/vol; 0.25–0.35 g/mL) were the best achieved (McDonald et al. 2006; Sibrell and Watten 2003). Hence, reversing the addition so that the ARD is dosed to the carbonate in a continuous-batch system potentially provides pre-conditioning, controlled-dosing, and slow neutralisation rates (controlled by the mineralogy), all of which should contribute to producing a high density sludge (Bosman 1974; Georgaki et al. 2004, Yong Gan et al. 2005).

The use of axial mixing (mixing in the centre of a tank to draw water down and outwards from the centre) to suspend limestone into a batch treatment system has been previously demonstrated to be low-energy and low-maintenance, and to have a low initial capital outlay (Oldshue and Herbst 1992). Axial mixers also provide a means of lifting carbonate particles into suspension, and inter-particle collisions may prevent some armour coatings from forming. This study investigates using an active oxidation chamber in a three-stage axial-mixed neutralisation of Fe-rich ARD using a waste carbonate (dolomite and magnesite).

Methods

ARD sourced from the Savage River Mine Old Tailings Dam, West Seep (Savage River, Tasmania; Fig. 1) was used in this study. This is the greatest acidity source on the Savage River lease (mostly due to the high dissolved iron concentrations). The Eh and pH (+240 mV at pH 2.4) suggests that much of the dissolved iron is in a reduced Fe(II) state in the sample; Eh would typically be +500 mV for oxidised Fe-rich ARD. ARD was collected from the tailings dam seepage using several black polypropylene Jerry cans, excluding the air gap as much possible by filling the container to the absolute brim before sealing it. The sample was transferred to the lab and testing was started within 24 h of sample collection. The ARD was a slightly yellow tinged, but clear, and over the time of testing, no discernable colour change or iron precipitation occurred. The carbonate was sourced from a deposit in the Savage River Mine North Pit. A representative 10 t sample was crushed to 20 mm, then sub-sampled and ground in a ring mill.

A schematic of the carbonate reactor is presented in Fig. 1. Two identical perspex jars (95 mm diameter × 180 mm high) were used as reactor vessels. Each jar had three vertical baffles (9 mm wide) fitted to enhance mixing. Mixers (12 V cordless drills with a 12 V motor speed control circuit) were computer-controlled using a PCI-DAS6025 data acquisition card and Matlab® Data Acquisition Toolbox software. The computer also logged pump rate, pH, and temperature (industrial pH probe (Endress + Hauser CPF81-M11C8) and transmitter (Endress + Hausser Liquisys CPM 253)) every 10 s for later analysis, and regulated the acid drainage flow rate through the reactors. Dissolved oxygen was measured manually with a field meter (WTW Oximeter 320 with Probe #325). The oxidation chamber was a plastic container (250 mm wide × 360 mm long with 7 L capacity). The oxidation chamber was aerated using a glass aquarium air stone and standard aquarium air pump, with a piece of stretched glass capillary to reduce aeration rates close to that expected at scale up.

Both Cell 1 and Cell 2 contained 125 g of carbonate. During operation, both cells were subjected to a 20 min

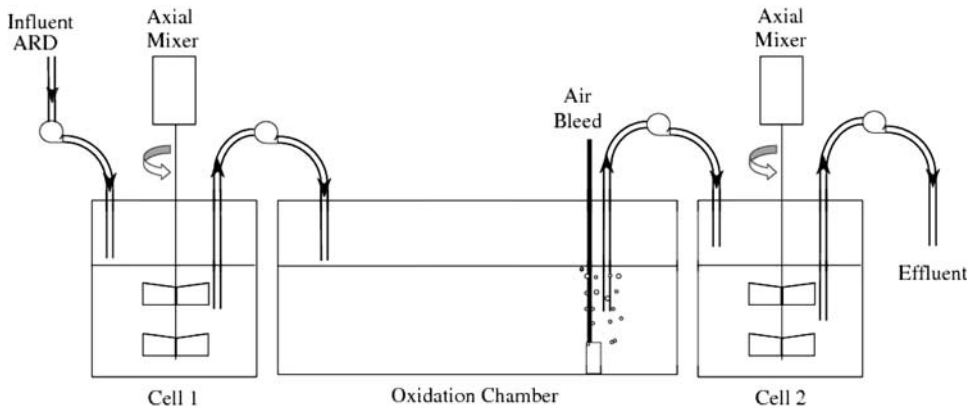

Fig. 1 Schematic of the reactor (not to scale)

mixing phase where neutralisation occurred, followed by a 10 min settling phase. During the last two minutes of the settling phase, water from each cell was pumped off from the surface of the cell; the decant from Cell 1 was pumped to the oxidation chamber, and the decant from Cell 2 was pumped to an effluent storage container. Cell 1 received ARD continuously during the mixing phase but not during the settling phase. A 700 mL reservoir of water and carbonate was retained in Cell 1 at all times by fixing the exit tube at 90 mm depth (the 700 mL point in the jar).

Water in the oxidation chamber was bubbled with air continuously, and pumped to Cell 2 during the first three minutes of the 20 min mixing phase. Placing the air stone directly under the exit tube from the oxidation chamber prevented meniscus formation and ensured consistency of volume delivered. The decant water from Cell 2 was pumped to an effluent storage container during the last two minutes of the settling phase.

During operation, the pH of Cell 2 was maintained at a target pH of 6.3 by controlling the influent ARD flow rate into cell 1. Every 30 min, prior to decanting if the pH in Cell 2 was meeting the target of 6.3, then flow remained constant; if the pH in Cell 2 fell below 6.3, flow was adjusted down; and if the pH was greater than 6.4, then flow was increased. A target pH of 6.3 was chosen because some fine-grained carbonates were expected to remain suspended and carry over into the effluent storage container, and further raise the pH. The water in each effluent storage container was allowed to settle for at least 3 days before analysis.

Analytical Methods

X-ray diffraction profiles of the sludges and waste carbonate rock were collected using a Philips X-ray diffractometer system (PW 1729 generator, PW 1050 goniometer, with nickel-filtered copper radiation at 40 kV/30 mA, a graphite monochromator (PW1752), sample spinner and a proportional detector (sealed gas filled, PW1711) calibrated with an internal standard of natural quartz. The system was computer-controlled (PW 1710 microprocessor driven by the Diffraction Technology software: "Visual XRD v 2.6" and CSIRO software: PW1710 for Windows" with plotting software "XPLOT for Windows" (CSIRO), and "Traces v.5.1" (Diffraction Technology). The samples were prepared by drying and grinding to $<\approx$ 10–75 μm. The semi-quantitative mineralogy was determined by manual search-match methods, using a series of prepared standards.

Particle size was determined using a Malvern Micro-P Model–33850/18 laser particle analyser. Samples were analysed using the 'Polydisperse Analysis Mode' with a mono-modal analysis model, and 'Fraunhoffer' presentation. Sample suspensions were placed in a 600 mL sample beaker, and the pump speed set at 3,000 rpm. A blank sample of dispersant and water was run, and three repeat analyses of the sample made. Repeat analyses of the sample were then averaged, and the average grain size exported to Excel.

The acid neutralising capacity (ANC) of the waste carbonate rock was determined by reacting a sample with a known quantity of standardised hydrochloric acid, and heating until CO_2 evolution ceased (based on the method of (Harries (1997) after Sobek et al. (1978). This was then diluted with distilled H_2O, boiled, and then cooled. A back-titration with standardised NaOH determined the amount of HCl consumed.

Water chemistry analyses were based on (APHA 1998) methods and included:

- 1102-Water Acidity by APHA Method 2310 using Metrohm 716 DMS Titrino,
- 1101-Water Alkalinity by APHA Method 2320/4500 using Metrohm 716 DMS Titrino,
- 1301-Water Metals in Water by APHA Method 3010/3120 3120 using Varian Vista AX ICP-AES,
- 1103-Water Anions by Ion Chromatograph APHA Method 4110C using Dionex ICS-3000 (CO_2 Ion Chromatograph),
- 1302-Water Major Cations in Water by APHA Method 3030/3120 using Varian Vista AX ICP-AES,
- 1002-Water Conductivity by APHA Method 2510 using Cyberscan 500,
- 1001-Water pH in Water by APHA Method 4500-H using Orion Model 290, and
- 1011-Water Solids, Total Suspended 0.45 μm Filtration.

Sludge density measurements were made by allowing the sludge to settle for 3 days; the water was decanted off to the water-sediment interface. The subsequent wet sludge was transferred to a pre-weighed measuring cylinder and the volume of the wet sludge was measured. The sludge was then oven dried at 105°C for 48 h or until constant weight was maintained. Cylinders were then equilibrated at room temperature in a desiccator, and re-weighed to attain the mass of solids in the cylinder. The mass gain was then divided by the total volume to provide the sludge density as a % wt/vol, or as g/mL.

Results

Figure 2 shows the results of the laser particle size analysis; the grain size of the crushed materials was mostly (85%) <38 μm with a substantial proportion (25%) of the waste carbonate <1.2 μm. Replicate samples indicate that

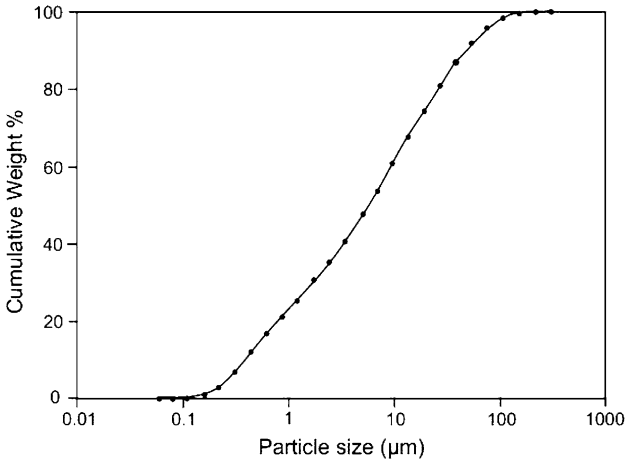

Fig. 2 Waste carbonate rock particle size distribution used in this work. The fine grained nature of the carbonates will tend to preclude armouring and allow complete dissolution to occur on the solubility kinetics of the minerals present

individual analyses varied less than 5%, suggesting that the data are highly reproducible. Such fine grain sizes for the carbonates suggested that armouring of the particles was unlikely to be a substantial problem. In addition, the XRD analyses indicated that dolomite dominates the mineralogy of these carbonates, with considerable magnesite and minor calcite (Table 2). The presence of these minerals mean that the neutralisation rate will be slower than if calcite alone was used (Stumm and Morgan 1996), but that a denser type of sludge should be produced.

The acid neutralisation rate as % per day is defined as:

$$\text{Reaction rate} = \frac{\text{Acidity load into the reactor per day } (CaCO_3 \text{ equiv}) \times 100}{\text{ANC initially loaded in both cells of the reactor } (CaCO_3 \text{ equiv})}. \quad (9)$$

The acid neutralisation rate of the carbonate in the reactor was initially 8% of the ANC/day, which gradually declined to a more consistent value of 3.25% of the ANC/day, from the time about 30% of the carbonate acid-neutralising capacity was consumed (Fig. 3). The higher initial rate of carbonate consumption (alkalinity release and acid neutralisation) probably reflects the consumption of the finer mineral fragments, the <1.2 μm fraction; the coarser fractions then supply a much more uniform rate of alkalinity. The more uniform alkalinity supply is coming mostly from the dolomite rather than the magnesite, because in the residue analyses (Table 2), appreciable magnesite remained, even in the first reaction cell solids, which bore the brunt of the acid attack. Similarly, the alkalinity consumption rate varies along with the rate of pumping of influent into Cell 1 (Fig. 3), from nearly 5 mL/min to about 1.5 mL/min.

Table 2 Characteristics of waste rock carbonate and the sludges produced

	Weight (g)	Sludge volume (mL)	Sludge density % wt/vol (g/mL)	ANC g $CaCO_3$ equiv[a]	Magnesite % by wt	Dolomite % by wt	Calcite % by wt	Amorphous FeO % by wt	Gypsum[b] % by wt	Other % by wt[c]
					XRD data[d]					
Starter carbonate in each cell[e]	125	–		99	30	42	1			27
Cell 1 sludge	118.4	222	53 (0.53)	27	24	4	nd	32	16	24
Oxidation chamber sludge	13.3	43	31 (0.31)	1	9	2	nd	31	48	10
Cell 2 sludge	126.7	159	80 (0.8)	85	22	41	nd	7	11	19
Effluent sludge	36	–	–	–	–	–	–	–	–	–

[a] ANC (acid neutralising capacity) measured using APHA (1998) methods. The proportion of ANC consumed is calculated from the initial total ANC = 99 g

[b] Gypsum was detected in the dehydrated form, bassanite, which is created when the sludge is dried at temperatures > 50°C

[c] 27% of the waste carbonate rock was non-reactive components including quartz (8%), chlorite (8%), serpentine (3%) and 8% (others), and is also found in the sludge

[d] Results of XRD analysis of the residual materials measure by semi-quantitative methods, and using $Cu_{K\alpha}$ radiation

[e] Two cells containing 125 g waste carbonate rock gives a total of 250 g of waste carbonate rock in the reactor

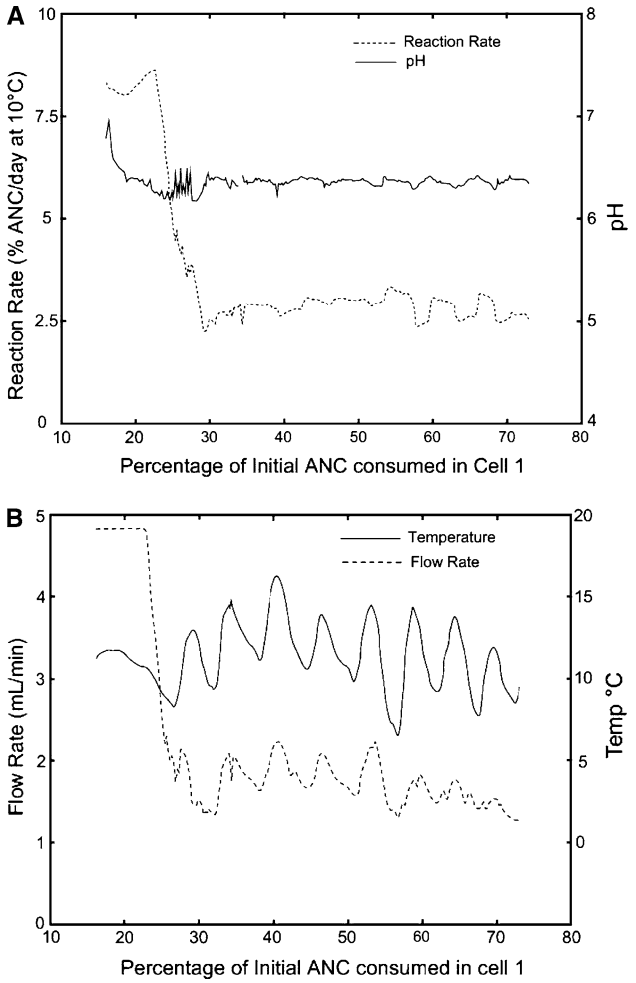

Fig. 3 Variation of the ANC consumption rate in Cell 1 and Cell 2 pH. Cell 2 is plotted as a function of proportion of the initial 99 g ANC consumed in Reaction Cell 1. Note that after initial high reaction rates in the first 30% of alkalinity consumption, flow and temperature become relational

Table 3 pH and acidity observations before and after treatment in the reactor

	pH	Sulphate, mg/L	Acidity to pH 7 mg/L $CaCO_3$ equiv
Influent ARD ($n = 7$)	2.4	6,300	2,980
Effluent ($n = 7$)	7.5	4,500	0
% Removal	na	29	100

During the treatment of the ARD, the pH rose to 7.5 (in the effluent storage container); at this pH, all acidity was considered to have been removed. Coincidentally, the release of Ca from the carbonates caused a 29% reduction in sulphate concentrations (Table 3) due to gypsum precipitation (Table 2). Although the pH in each effluent storage container was consistently close to 7.5 for the duration of the trial, the controlled pH in Cell 2 remained within the target of 6.3–6.4 (Table 4). This suggests that some of the very fine carbonates (Fig. 2) in Reaction Cell 2 carried over with the discharge waters to buffer the effluent storage container. This strongly affected metal solubility; after treatment, Al, Fe, Cu, and Cd concentrations in the ARD were all reduced to below detection limits, and Zn concentrations decreased by more than 70% (Table 5). Ca, Mg, Cl, K, Na, and Mn concentrations increased (Table 5).

The sludge formed in both reaction cells and in the oxidation chamber contained a substantial quantity of iron oxides and gypsum (Table 2). The sludge density was highest in Cell 2, indicating that the density was mostly because of unreacted carbonates (approximately 90% of the carbonates remained). In Cell 1, only 10% of the dolomite and about 80% of the magnesite from the carbonate remained in the sludge (Table 2), and the dolomite and magnesite made up 28% of the sludge material, whereas they were 72% of the original carbonate material.

The alkalinity consumed in each cell can be calculated by subtracting the alkalinity remaining in the sludge from the alkalinity in the initial carbonate. For Cell 1, there was the initial 99.8 g $CaCO_3$ equiv minus the 26.6 g $CaCO_3$ equiv remaining (Table 2), giving a consumption of 73.2 g $CaCO_3$ equiv. Similarly, for Cell 2, the initial 98.8 g of $CaCO_3$ equiv was reduced to 84.8 g $CaCO_3$ equiv (Table 2), a consumption of 14.0 g of alkalinity. This gives a total consumption of 87.2 g $CaCO_3$ equiv from both cells. Given that the total volume of effluent treated was 29.2 L, and influent acidity was 2,980 mg $CaCO_3$ equiv/L to pH 7 (Table 2), then the total alkalinity required to treat the water would be 87.0 g $CaCO_3$ equiv to pH 7. These data also indicate that there is about a one-to-one relationship between acidity treated and alkalinity consumed.

On scale up, there is the option of transferring the unused carbonate in Cell 2 to Cell 1 and recharging Cell 2 with fresh material, thereby setting up a counter-current system. This may increase overall efficiency of the system because the largely unused ANC in Cell 2 in normal flow would become the primary contact point in the reversed flow. However, the data (Table 2) indicates that the current system is about 70% efficient for Cell 1 (27 g of $CaCO_3$ equiv ANC remaining from the 99 g of $CaCO_3$ equiv ANC added).

Discussion

The results show that at bench-scale, this design can effectively facilitate neutralisation, with sufficient removal of heavy metals via precipitation, and that the sludge produced has characteristics favourable for disposal. The removal of the metal contaminants from the Fe-rich ARD from the Savage River ARD (Old Tailings Dam seeps)

Table 4 Dissolved oxygen and pH in Cells 1 and 2, and the oxidation chamber of the reactor

Days run	Dissolved oxygen (% Saturation)			pH			
	Cell 1	Oxidation chamber	Cell 2	Cell 1	Oxidation chamber	Cell 2	Settled effluent
0.1	90	75	20	4.7	5.88	6.42	7.7
1.2	67	80	59	5.02	5.09	6.32	7.4
2.1	70	85	60	5	5.2	6.3	
2.9	82	88	67	4.87	5.13	6.32	7.6
4.0	90	85	72	4.7	5.23	6.34	7.6
5.1	86	–	65	4.6	5.06	6.3	7.5
6.2	93	90	71	4.41	4.95	6.45	7.5
7.2	95	85	72	4.4	4.7	6.45	
8.9	96	90	79	3.03	3.95	6.41	7.5

appears to follow generally accepted pathways for ARD treated with lime addition. That is, as pH rises, metals become less soluble by the formation of amphoteric metal hydroxides (Eary 1999), despite the primary pH adjuster being a carbonate (Lottermoser 2003). The order of metal removals seen (Table 4) are consistent with the pKa of hydration of the metals:

- Fe^{3+} and Al^{3+} were removed in the first reaction cell as pH rises to about 4.5;
- Fe^{2+} and Cu^{2+} were removed in the oxidation chamber as pH increased to about 5.5 and oxidation was allowed to occur under oxygen-saturated conditions; and then
- Zn^{2+} was removed as the pH of the effluent increased to about pH 7.5.

However, Ni^{2+}, Co^{2+}, and Mn^{2+} remained in solution because the pH was not sufficiently high to exceed the pKa of hydration and allow removal as a hydroxide (Alyward and Findlay 1989; Eary 1999; Tables 1, 4, and 5).

Increases in Ca, Mg, and Mn concentrations (Table 5) were from the dissolution of the mixed magnesite-dolomite-calcite carbonates; Mn can readily substitute for Ca in a carbonate structure. This was associated with a substantial decrease in the sulphate concentration (Table 5), due to the precipitation of gypsum (Table 2) and/or mixed aluminium hydroxy-sulphates (e.g. alunite). Observed increases in Na, Cl, and K concentrations (Table 5) were probably from the natural variation of the analyses at the low concentrations measured.

The pH in the effluent samples was well above pH 7 (targeted end-point), even though the Cell 2 decant pH leaving the reactor was around 6.3. The pH rise in the effluent samples suggests that fines in the decant water continued to add alkalinity and/or there was a loss of CO_2. It is likely that both would occur in a mine pit or dam if the technology was scaled up, although the magnitude of the effect may change. The fact that the mine pits are deeper will mean that the fines will be suspended in the water column longer. This will increase the reaction of the fines in the water column. Once settled, however, the effect of the fines will be reduced compared to this pilot reactor, due to the lower ratio of bottom surface area to the volume of water above. The large hydraulic retention time in the pit will permit CO_2 concentrations to approach equilibrium with the atmosphere.

Several metals present in the Savage River ARD (Old Tailings Dam seeps used in this work) are of concern for toxicity for species diversity and abundance in the Savage River, in particular Al and Cu (Davies et al. 2001). The process described here decreased the concentrations of Al, Fe, Cu, and Cd to below detection limits (Table 4), although some trace metals, including Co, Mn, Ni, and Zn (Table 4), remained above the 95% protection ANZECC (2000) guidelines. The concentrations of these constituents are not significant for the protection of target species at Savage River (Davies et al. 2001), but may be of concern at other sites. Despite the higher concentrations, the toxicity effects of these trace metals are further ameliorated by the increase in water hardness (Ca and Mg concentrations; Table 5), decreasing their effective toxicity to target species (Davies et al. 2001). The effluent waters from the plant contain appreciable quantities of Co^{2+} (Table 4), which accelerates Fe oxidation.

Iron concentrations decreased from 856,000 μg/L to <20 μg/L in the discharge effluents (Table 4). It is therefore very likely that Fe(II) oxidation rates are substantially higher than those predicted by either Eqs. 7 or 8. Furthermore, the constant bleed of O_2 via the oxidation chamber also means that the abiotic oxidation rate via Eq. 8 remains high because $[O_2]$ rarely falls below 4×10^{-4} mol/L (80% of saturation at 8 mg/L; Table 3). There is a loss of O_2 saturation in Cell 2, typically <60% saturation or $<3 \times 10^{-4}$ mol/L. This indicates that substantial oxidation occurs in Cell 2. The pH in Cell 2 rises

Table 5 Concentrations of metals of environmental significance at different points in the reactor

	Ca Total (mg/L)	Cl Total (mg/L)	K Total (mg/L)	Mg Total (mg/L)	Mn Total (mg/L)	Al Total (µg/L)	Co Total (µg/L)	Cu Total (µg/L)	Fe Total (µg/L)	Fe Dissolved (µg/L)	Ni Total (µg/L)	Zn Total (µg/L)	TSS mg/L
Influent ARD ($n = 7$)	375	16	16	498	11.5	7,220	5,490	264	856,000	852,000	3,660	1,190	3
Cell 1 ($n = 2$)	NA	NA	NA	NA	NA	8,235	5,655	392	298,000	221,500	3,795	1,380	–
Oxidation chamber ($n = 2$)	NA	NA	NA	NA	NA	1,660	5,260	159	121,500	112,500	3,505	1,015	–
Cell 2 decant ($n = 2$)	NA	NA	NA	NA	NA	902	5,445	21	19,805	NA	3,560	484	–
% Removal prior to settling	NA	NA	NA	NA	NA	*88*	*1*	*92*	*98*	–	*3*	*59*	–
Effluent ($n = 7$)	515	21	30	770	15	<20	5,236	2	181	<20	3,324	265	<1
% Removal after settling	37.5[a]	34.5[a]	88.5[a]	55.5[a]	28.5[a]	≈100	5	99	≈ 100	≈ 100	9	78	–

Metal concentrations are expressed as total values only, as concentrations of dissolved metals were not significantly different, as supported by the low TSS values. Note that As and Cr were below detection in both the influent and effluent: As (<5 µg/L), Cr (<1 µg/L). Apart from Fe, dissolved metals are not reported because concentrations of these were not significantly different to total metal concentrations, except for undetectable dissolved Fe in the influent and effluent; this is supported by the low TSS values

Significant according to the toxicological study of (Davies et al. 2001); note that As and Cr were below detection in both the influent and effluent: As (<5 µg/L), Cr (<1 µg/L)

[a] Recorded increase in concentration

from about 5 to 6.3, which according to Eq. 7 will effectively increase oxidation rates by an order of magnitude or more.

Calculations of the Fe oxidation rate using rate constants generated by others (e.g. Kirby and Elder Brady 1998; Pesic et al. 1989; Stumm and Morgan 1996), suggests that the homogeneous oxidation rate (Eq. 6) in Cell 1 should be in the range of 1.14×10^{-2} to 1.34×10^{-4} mol/L/s.; instead, the heterogenic oxidation rate (Eq. 7) ranges from 2.82×10^{-5} to 3.32×10^{-7} mol/L/s. The data suggests that the removal rate for Fe in Cell 1 is 3.03×10^{-7} mol/L/s and 5.2×10^{-8} mol/L/s for the oxidation chamber. Hence, the rate for Fe removal in cell 1 is much more likely to be controlled by the heterogenic oxidation rate (Eq. 7) than the homogeneous oxidation rate (Eq. 6). This is likely because the denominator of the heterogenic rate is more readily controlled by the alkalinity supply to the system from carbonate dissolution.

The waste carbonate rock used was approximately a 3:2 mixture of dolomite and magnesite, with minor amounts of calcite (Table 2). The trial stopped when the pH in Cell 1 began to drop considerably (Table 4), indicating a near exhaustion of the Cell 1 ANC, or when the ANC supply fell consistently to about 2.5% of ANC/day. This suggests the nearly complete exhaustion of dolomite from the ANC; the ANC could only be supplied by the residual magnesite or silicate minerals (Table 2). The ANC of the remaining Cell 1 sludge represents about 30% of the initial ANC (Table 3). The reactor consumed alkalinity at rate of about 3.25% of the total neutralising capacity per day (Fig. 3). Initially, the rate was substantially higher than this, probably due to the presence of some very fine-grained and highly reactive carbonates. As neutralisation progressed, the ANC consumption rate fell to a more constant value. This is probably an effect of grain size, where the finest grains are consumed first (or physically lost with the effluent early); about 25% of the carbonates were less than 1.2 µm (Fig. 2).

Recalculating this rate (Fig. 3) gives a dissolution rate of 3.724×10^{-7} mol/L/s, which is cf. 3 orders of magnitude greater than predicted by Stumm and Morgan (1996) for the exit pH of 4.5 from Cell 1. However, the pH for ARD is a poor substitute for the alkalinity consumption; titratable acidity is more relevant because acidity is stored as positive metal cations (e.g. Fe^{3+} and Fe^{2+}). Given that carbonate neutralises $2H^+$ means that the H^+ consumption rate should be 7.448×10^{-7} mol/L/s; the calculated H^+ consumption rate is 7.947×10^{-7} mol/L/s. Because the alkalinity supply rate and the Fe oxidation rate are very similar, it is unlikely that the heterogeneic oxidation of Fe(II) in the waters will limit the operation of this reactor. It is more likely that carbonate dissolution rates, especially for the magnesite, will have far more influence on the

operational efficiency. In addition, the Cell 1 sludge is dominated by magnesite (Table 2), indicating that the dolomite and calcite present in the waste carbonate rock were more reactive and almost entirely consumed in Cell 1 (Table 2). This dissolution of the carbonates is in accordance with the published findings for individual carbonates (Stumm and Morgan 1996; cf. Fig. 13.14). In addition, the observation that the dolomite is neutralising more ARD than magnesite is also consistent with the field and experimental observations from karst systems (Household et al. 1999).

The rise in pH in the oxidation chamber despite iron oxidation and precipitation and mineralogy of the sludge in the oxidation chamber indicates that some of the carbonates from reaction Cell 1 are being carried over. This is likely because the settling time in Cell 1 was insufficient to fully remove the fine suspended material. Similarly, fine-grained highly reactive material in Cell 2 is being carried over and is buffering the effluent. Effectively all of the fine-grained highly reactive-material in Cell 2 was already consumed, so a more stable supply of alkalinity could be maintained from the residual. This should then allow the flow to be reversed so that Cell 2 becomes Cell 1 and visa versa, effectively setting up a two-stage counter-current system that would more fully utilise the alkalinity in the system and thereby improve overall efficiency.

Notwithstanding the excellent overall removal of iron, the soluble iron levels were reduced by only about 50% in the oxidation chamber (Table 4). This suggests that the oxidation chamber efficiency can be improved. The hydraulic retention time in the chamber varied between 2 and 4 days, but averaged about 2.5 days. A longer hydraulic retention time (increasing the relative chamber size) could improve iron removal. A greater agitation in the oxidation chamber may also improve oxidation rate by suspending the ferric oxides and effectively increasing the reactive area for oxidation.

In this trial, the reactor was run with fresh carbonate in both Cell 1 and Cell 2, which primes the reactor. However, in subsequent runs, Cell 2 sludge will be recycled by reversing the direction of flow in the reactor, as discussed above. Fresh carbonate will be added to Cell 2 (formerly Cell 1). Although similar systems are "notorious" for producing "voluminous, low-density" sludge (Sibrell and Watten 2003), this design produced a high density sludge of 53% (wt/vol.) in Cell 1, about twice as dense as the best reported by Sibrell and Watten (2003). The residual alkalinity in the sludge provided by the magnesite is a favourable characteristic and the results of McDonald et al. (2006) indicates that this magnesite will very likely contribute to the long-term stability of the sludge.

Conclusion

This study showed that axial mixing in reaction cells with an intermediate oxidation chamber has great promise for neutralising iron-rich ARD; the system also produced a high-density sludge. The results can be explained with known chemical kinetics. Iron removal from the system is explainable through heterogeneous oxidation, which is limited by the supply of alkalinity to consume H^+. More importantly, the system described has the capacity to utilise on-site "waste" carbonates prepared using existing autogenous and ball mills at the mine site, though this can only be done after mine operations cease and the mill becomes available. This is convenient as alkalinity in the mine tailings currently treat the Old Tailings Dam seepages. The use of the waste carbonate rock offers large potential cost savings over conventional reagents, such as hydrated lime or magnesium oxide, because there is little net cost of excavation and delivery (these costs are accounted for in the cost of ore recovery) and no calcination is required.

The low-tech nature of the treatment plant and the fact that acid neutralisation and Fe oxidation appear to be self-regulating provides a potential long-term operational advantage as well. In addition, the sludge can be disposed of to the pits because of the residual buffering capacity in the solids.

Acknowledgments We would like to thank Department of Tourism, Arts and the Environment, Tasmania for permission to publish this work. Mineral resources Tasmania have supported the project through the provision of infrastructure and assistance from the staff at the core store. Lois Koehnken, Rob Dineen, Shane Underwood and Jeff Taylor have also provided significant technical expertise and support to the project. Australian Bulk Minerals staff, especially Stephen Kent, Bruce Hutchison and Tony Ferguson has also provided expertise and consistent support to the ongoing development of the neutralisation technologies.

References

ANZECC (2000) Australian and New Zealand guidelines for fresh and marine water quality, 4A. Australian and New Zealand Environment and Conservation Council

APHA (1998) Standard methods for the examination of water and wastewater. American Public Health Association, Washington DC, USA, 356 pp

Aylward GH, Findlay TJV (1989) SI chemical data. Wiley, Hong Kong, China, 136 pp

Berner RA, Morse JM (1974) Dissolution kinetics of calcium carbonate in seawater, IV. Theory of calcite dissolution. Am J Sci 274:108–134

Bosman DJ (1974) Improved densification of sludge from neutralized acid mine drainage. J S Afr Inst Min Metall 74:340–348

Busenberg E, Plummer LN (1986) A comparative study of the dissolution and crystal growth kinetics of calcite and aragonite. USGS Bull 1578:816–837

Chou L, Garrels RM, Wallast R (1989) Comparative study of the kinetics and mechanisms of dissolution of carbonate minerals. Chem Geol 78:269–282

Davies PE, Eriksen R, Cook LSJ, Risdon ML (2001) Toxicological evaluation of acid drainage waters and treatment options at Savage River, western Tasmania: Savage River Rehabilitation Program. Report to the Dept of Primary Industries, Water and Environment, Tasmania, Freshwater systems, Hobart, Australia, 136 pp

Dempsey BA, Roscoe HC, Ames R, Hedin R, Jeon B (2001) Ferrous oxidation chemistry in passive abiotic systems for the treatment of mine drainage. Geochem Explor Environ Anal 1:81–88

Eary LE (1999) Geochemical and equilibrium trends in mine pit lakes. Appl Geochem 14(8):963–988

Evangelou VP (2000) Geochemistry, water and soils. CRC Press, Bocca Raton, 575 pp

Georgaki I, Dudeney AWL, Monhemius AJ (2004) Characterisation of iron-rich sludge: correlations between reactivity, density and structure. Miner Eng 17:305–316

Harries J (1997) Acid mine drainage in Australia: its extent and potential future liability. Supervising Scientists Report 125, Supervising Scientists, Canberra, Australia, 94 pp

Household I, Calver C, Sharples C (1999) Magnesite Karst in Northwest Tasmania. Unpublished report to Div of Investment, Trade and Development, Dept of State Development, Tasmania, Australia, 123 pp

Johnson DB, Hallberg KB (2005) Acid mine drainage remediation options: a review. Sci Total Environ 338:3–14

Kirby CS, Elder Brady JA (1999) Field determination of Fe^{2+} oxidation rates in acid mine drainage using a continuously-stirred tank reactor. Appl Geochem 13(4):509–520

Kirby CS, Thomas HM et al (1999) Relative contributions of abiotic and biological factors in Fe(II) oxidation in mine drainage. Appl Geochem 14(4):511–530

Koehnken L Ray D (1999) Water quality on the ABM lease and in the Savage River – a review for the Savage River Rehabilitation Project (SRRP), Hobart, Australia, DPIWE, 21 pp

Lide DR (2003) Handbook of chemistry and physics. CRC Press, Boca Raton, 2553 pp

Lottermoser BG (2003) Mine wastes: characterization, treatment, and environmental impacts. Springer Verlag, Berlin, 277 pp

McDonald D, Webb J, Taylor J (2006) Chemical stability of acid rock drainage treatment sludge and implications for sludge management. Environ Sci Technol 40:1984–1990

Oldshue J, Herbst N (1992) A guide to fluid mixing. Lightnin, New York, 153 pp

Parker G, Robertson A (1999) Acid drainage. Occasional Paper # 11, Australian Minerals and Energy Environment Foundation, Melbourne, Australia, 227 pp

Pesic B, Olivier DJ, Wichlacz P (1989) An electrochemical method of measuring the oxidation rate of ferrous to ferric iron with oxygen in the presence of *T. ferrooxidans*. Biotechnol Bioeng 33:428–439

Plummer LN, Wigley TML, Parkhurst DL (1978) The kinetics of calcite dissolution in CO_2–water systems at 5° to 60°C and 0.0 to 1.0 atm CO_2. Am J Sci 278:179–216

Sibrell PL, Watten BJ (2003) Evaluation of sludge produced by limestone neutralization of AMD at the Friendship Hill National Historic Site. Proceedings, National Meeting of the American Soc of mining and reclamation and the 9th Billings Land Reclamation Symp, Billings MT, ASMR, Lexington, KY, USA, pp 1151–1169

Skousen J, Rose A, Geidel G, Foreman J, Evans R, Hellier W, Members of the Avoidance and Remediation Working Group (1998) Handbook of technologies for avoidance and remediation of acid mine drainage. The National Mine Land Reclamation Center, Morgantown, WV, USA, 131 pp

Skousen J, Hilton T, Faulkner B, (2005) Overview of acid mine drainage treatment with chemicals. West Virginia Univ and National Mine Land Reclamation Center, Morgantown, WV, USA. http://www.wvu.edu/~agexten/landrec/chemtrt.htm

Sobek A, Schuller W, Freeman J, Smith R (1978) Field and laboratory methods applicable to overburdens and mine soils. EPA 600/2-78-054, US Dept of Commerce, NTIS, Springfield, VA, USA, 204 pp

Stumm W, Morgan JJ (1996) Aquatic chemistry, chemical equilibria and rates in natural waters. Wiley, New York, 1022 pp

Taylor G (1999) Acid drainage. Austr Geol 110:32–33

Watten BJ, Sibrell PL et al (2004) Effect of acidity and elevated P_{CO_2} on acid neutralization within pulsed limestone bed reactors receiving coal mine drainage. Environ Eng Sci 21(6):786–802

Yong Gan W, Selomulya C, Tapsell G, Amal R (2005) Densification of iron(III) sludge in neutralization. Int J Miner Process 76(3):149–162